Image Cover Sheet

CLASSIFICATION	SYSTEM NUMBER 155037
UNCLASSIFIED	

TITLE

CYCLOSTATIONARY SPECTRAL ANALYSIS OF TYPICAL SATCOM SIGNALS USING THE FFT ACCUMULATION METHOD

System Number:

Patron Number:

Requester:

Notes:

DSIS Use only:

Deliver to: FF

National Défense
Defence nationale

CYCLOSTATIONARY SPECTRAL ANALYSIS OF TYPICAL SATCOM SIGNALS USING THE FFT ACCUMULATION METHOD (U)

by

Caroline Tom

DEFENCE RESEARCH ESTABLISHMENT OTTAWA
REPORT NO. 1280

Canada

December 1995
Ottawa

National   Défense
Defence   nationale

CYCLOSTATIONARY SPECTRAL ANALYSIS OF TYPICAL SATCOM SIGNALS USING THE FFT ACCUMULATION METHOD (U)

by

Caroline Tom
MIL SAT Communications Group
Space Systems and Technology Section

DEFENCE RESEARCH ESTABLISHMENT OTTAWA
REPORT NO. 1280

ABSTRACT

The suitability of cyclostationary spectral analysis for the detection and identification of typical Satcom signals is examined. An overview of the general equations for cyclostationary spectral analysis is presented. The cyclic spectrum is derived for some common Satcom modulation schemes. Cyclic spectrum estimation techniques are described with particular emphasis on the time-smoothed approach. Key aspects of a computationally-efficient algorithm for computing the cyclic spectrum estimates, called the "Fast Fourier Transform (FFT) Accumulation Method" (FAM) are outlined. The FAM algorithm is implemented on a Digital Signal Processor/Personal Computer (DSP/PC) board containing a TMS320c51 processor chip and used to compute the cyclic spectrum for various phase-shift-keyed (PSK) and spread spectrum waveforms. The results are presented and discussed.

RÉSUMÉ

Ce rapport examine la pertinence de l'analyse du spectre cyclostationnaire pour la détection et l'identification des signaux typiques dans la communication par satellite. Les équations générales pour l'analyse du spectre cyclostationnaire sont presentées en résumé. Le spectre cyclique est derivé pour quelques exemples des modulations utilisées dans la communication par satellite. Une description des techniques de l'estimation du spectre cyclique est fournie en soulignant la méthode de la moyenne du temps. Les aspects importants d'un algorithme efficace en nombre d'opérations pour l'estimation du spectre cyclique sont presentés. L'algorithme s'appelle "La Méthode de l'Accumulation des Transformés de Fourier Rapides" (FFT Accumulation Method). L'algorithme est mise en oeuvre sur un unité de traitement des signaux numériques, TMS320c51. Le spectre cyclique est evalué pour des signaux transmis par déplacement de phase et les signaux étalés de spectre. Les resultats sont presentés.

EXECUTIVE SUMMARY

With further increases in the number of satellites and in the deployment of both large and small terminals expected in order to meet Satcom requirements for military communications, the risk of electronic interference causing Satcom stress[1] is of concern. This has lead to a desire to develop effective techniques to monitor Satcom links for electronic interference. Cyclostationary spectral analysis is examined to determine its suitability for detection and identification of typical Satcom signals.

The underlying principle of cyclostationary spectral analysis involves treating signals under examination as cyclostationary processes. For signals with periodic features, the advantage of using a cyclostationary model is that non-zero correlation occurs between certain frequency components of the signal where the frequency separation is related to the periodicity of interest. The general equations for cyclostationary spectral analysis are the cyclic autocorrelation and the cyclic spectral density.

Estimates of the cyclic spectrum using a time-smoothed approach can be obtained as follows: frequency components for a signal $x(t)$ are evaluated over a time window, T_w, along the entire observation interval, Δt; at each window, two components are multiplied; and the resulting sequence of products is integrated over time. This process, however, requires significant computational resources. A computationally-efficient algorithm for cyclic spectrum estimation is called the "Fast Fourier Transform (FFT) Accumulation Method" (FAM). The FAM algorithm computes cyclic spectrum estimates a block at a time by performing an FFT on the product sequence rather than an integration. Decimation and data tapering windowing considerations also reduce the number of computations.

The FAM algorithm is implemented on a Digital Signal Processor/Personal Computer (DSP/PC) board containing a TMS320c51 processor chip and used to compute the cyclic spectrum for binary-phase-shift-keyed (BPSK), quadrature-phase-shift-keyed (QPSK), frequency-hopped/M-ary frequency-shift-keyed (FH/MFSK), and FH/phase-shift-keyed (FH/PSK) waveforms. Periodic components such as the carrier frequency, symbol rate and hop rate appear as distinct cycle frequency components in the cyclic spectrum. Results also demonstrate that two or more signals can be detected in the same band of interest. Further improvements in estimate reliability for this implementation can be achieved by considering longer observation times (i.e. collecting more data samples). In turn, strategies including parallel implementations, algorithm development, and making use of advances in computing power will help to minimize compromises in computation time.

---

[1]Stress refers to any reduction in communications capability [1]

PRECEDING PAGE BLANK

TABLE OF CONTENTS

LIST OF FIGURES

PRECEDING PAGE BLANK

1.0 INTRODUCTION

Satellite communication (Satcom) requirements for military communications have increased significantly in recent years due to a desire to increase and maximize system throughput and to implement higher bandwidth and mobile applications. Advances in these areas have led to an increase in the number of satellites as well as the deployment of both large and small Satcom terminals. A potential consequence of this trend is the increased risk of electronic interference. The effects of electronic interference on Satcom links include increased noise in the payload receiver or ground terminal, a reduction in available transponder power output, and may ultimately deny timely authorized accesses. A recent "The Technical Cooperation Program" (TTCP) STP-6 workshop report [1] acknowledged electronic interference as a major source of Satcom stress[1] and looked at potential solutions. Ideally, solutions which not only detect the interference, but isolate the interference from valid Satcom signals are preferred.

Since the development of the theoretical concepts by Gardner [2,3] in the early-to-mid 80s, extensive work has been carried out to explore the potential of cyclostationary spectral analysis for traditional signal processing tasks. Studies in potential cyclostationary spectral analysis applications include time-difference-of-arrival (TDOA) estimation [4], signal detection and identification [5-7], and parameter estimation [7,8]. The underlying principle of cyclostationary spectral analysis involves treating the signal under examination as a cyclostationary rather than stationary process. For signals with periodic features (e.g. digital communications signals), the advantage of using a cyclostationary model is that non-zero correlation is exhibited between certain frequency components when their frequency separation is related to the periodicity of interest.

A major drawback of cyclostationary spectral analysis techniques is the tremendous processing requirement. As a result, a comparable effort has been put forward to develop computationally-efficient algorithms for computing the cyclic spectrum estimates. These include both time- and frequency-smoothing approaches [3,9,10]. Of particular interest in this report is a time-smoothing algorithm called the "Fast Fourier Transform (FFT) Accumulation Method" (FAM) [10]. It takes advantage of the FFT to compute the cyclic spectrum estimates a block at a time. Decimation and data taper windowing considerations also contribute to the computational efficiency of the FAM algorithm.

Several reports relating to cyclostationary spectral analysis work at the Defence Research Establishment Ottawa (DREO) or by DREO scientists over the last 5 years have

---

[1]Stress refers to any reduction in communications capability

also illustrated the potential of cyclostationary spectral analysis for many applications. These include an examination of cyclic spectrum estimate computations and their implications in a signal search and detect environment [11], an implementation of a computationally-efficient algorithm for cyclic spectrum estimation [12], and a report featuring a real-time optoelectronic implementation of a new algorithm which is able to detect, separate, and characterize spread spectrum signals [13].

This report examines cyclostationary spectral analysis as it is applied to detection and identification of some common Satcom signals. An overview of the theory for cyclostationary spectral analysis is presented in Section 2.0. Cyclic spectral densities for phase-shift-keyed (PSK) and spread spectrum waveforms are derived. Section 3.0 describes the time-smoothed cyclic spectrum measurement technique and introduces key concepts of the FAM algorithm. Principal components of the experimental setup are identified in Section 4.0, including the FAM implementation on a TMS320c5x digital signal processor (DSP). Results of the FAM computations are presented in Section 5.0 for PSK, quadrature-phase-shift-keyed (QPSK), frequency-hopped/M-ary frequency-shift-keyed (FH/MFSK), and frequency-hopped/phase-shift-keyed (FH/PSK) waveforms.

2

2.0 CYCLOSTATIONARY SPECTRAL ANALYSIS THEORY OVERVIEW

Cyclostationary spectral analysis differs from conventional spectral analysis because, as the name implies, signals under examination are modelled as cyclostationary rather than stationary processes [3,8]. For the analysis of waveforms with some periodic feature(s), a key advantage of using a cyclostationary model is that non-zero correlation is exhibited between certain frequency components when their frequency separation is related to the periodicity of interest. The value of that frequency separation is referred to as the cycle frequency. The non-zero correlation characteristic is reflected in the **cyclic autocorrelation function**, denoted, $R_x^\alpha(\tau)$, and its frequency-domain equivalent, the **cyclic spectral density** or **cyclic spectrum**, $S_x^\alpha(f)$ [3,8,14]. These are the general equations for cyclostationary or cyclic spectral analysis. They are defined

$$R_x^\alpha(\tau) \triangleq \underset{T \to \infty}{Lim} \frac{1}{T} \int_{-\frac{T}{2}}^{\frac{T}{2}} x(t+\frac{\tau}{2})\, x^*(t-\frac{\tau}{2}) e^{-j2\pi\alpha t}\, dt \qquad (1)$$

and

$$S_x^\alpha(f) \triangleq \mathscr{F}\{R_x^\alpha(\tau)\} = \underset{T \to \infty}{Lim} \frac{1}{T} X_T(f+\frac{\alpha}{2}) X_T^*(f-\frac{\alpha}{2}) \qquad (2)$$

respectively, where $\alpha = cycle\ frequency$, $\mathscr{F}\{\cdot\} = Fourier\ transform\ operator$, and

$$X_T(f) \triangleq \int_{-T/2}^{T/2} x(u) e^{-j2\pi f u}\, du$$

The additional cycle frequency variable in **(2)** is reflected in a two-dimensional representation of $S_x^\alpha(f)$ referred to as the (f,α) or bifrequency plane (Figure 2.1(a)). For a bandlimited signal, the range of values of f and α for which $S_x^\alpha(f)$ exists is referred to as the region of support. Figure 2.1(b) illustrates the region of support for lowpass signals.

3

Figure 2.1 (a) Bifrequency plane (b) Region of support for lowpass signal
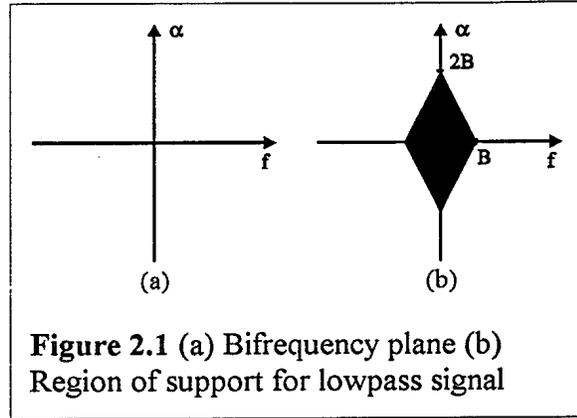
For waveforms which have undergone common signal processing operations (e.g. filtering, modulation), evaluation of **(1)** and **(2)** can be cumbersome. However, in [3,8] several properties or relationships are described which help simplify this task. One useful result is the expression of the cyclic autocorrelation for the product of two independent waveforms. It is shown [3,8], that for $x(t)=d(t)c(t)$,

$$R_x^\alpha(\tau) = \sum_\beta R_d^\beta(\tau) R_c^{\alpha-\beta}(\tau) \tag{3}$$

Thus, the cyclic autocorrelation of a product of two independent waveforms is given by the discrete convolution in cycle frequency of the independent cyclic autocorrelation functions. The cyclic spectrum is then given by

$$S_x^\alpha(f) = \int_{-\infty}^{\infty} \sum_\beta S_d^\beta(v) S_c^{\alpha-\beta}(f-v) dv \tag{4}$$

Note that the cyclic spectrum is continuous in f and discrete in α. The results of **(3)** and **(4)** are used to evaluate the cyclic spectrum of some typical Satcom signals.

2.1 Cyclostationary Spectral Analysis of Satcom Signals

Common Satcom signals may include PSK and QPSK modulations depending on data rate requirements. FSK modulation schemes may be used for low data rate applications and in cases where bandwidth efficiency is of less importance. In addition, direct sequence code division multiple access (CDMA), FH/MFSK and frequency-hopped DPSK (FH/DPSK) are now becoming more commonplace for a number of reasons, not the least of which is their robustness to electronic interference. For detection and identification applications, it is thus appropriate to individually examine the cyclic spectrum of these more typical Satcom signals.

2.1.1 PSK

Let the PSK signal be described by

$$x(t)=d(t)c(t)=d(t)\cos(2\pi f_o t + \phi_o)$$

where $d(t)$ is the data signal and $c(t)$ is the cosine or carrier term. Since $d(t)$ and $c(t)$ are independent time series, the cyclic autocorrelation of $x(t)$ may be given by (3). Applying the cyclic autocorrelation function definition, (1), to the cosine term $c(t)$ yields

$$R_c^{\alpha}(\tau)=\begin{cases} \frac{1}{2}\cos(2\pi f_o\tau); & \alpha=0 \\ \frac{1}{4}e^{\pm j2\phi_o}; & \alpha=\pm 2f_o \\ 0; & otherwise \end{cases}$$

The cyclic spectrum for the cosine term is hence given by

$$S_c^{\alpha}(f)=\begin{cases} \frac{1}{4}\delta(f\text{-}f_o)+\frac{1}{4}\delta(f\text{+}f_o); & \alpha=0 \\ \frac{1}{4}e^{\pm j2\phi_o}\delta(f); & \alpha=\pm 2f_o \\ 0; & otherwise \end{cases}$$

which consists of delta functions at the carrier frequency for $\alpha=0$ and at $f=0$ for $\alpha=\pm 2f_o$. The cyclic spectrum for $x(t)$ is then simply the cyclic spectrum of the data sequence, $d(t)$, replicated at the cosine term delta functions.

$$S_x^{\alpha}(f)=\begin{cases} \frac{1}{4}S_d^{\alpha}(f\text{-}f_o)+\frac{1}{4}S_d^{\alpha}(f\text{+}f_o); & \alpha=0 \\ \frac{1}{4}e^{\pm j2\phi_o}S_d^{\alpha}(f); & \alpha=\pm 2f_o \end{cases}$$

Now consider the data signal $d(t)$ which may also be rewritten as a time-sampled random data waveform, $a(t)$, with the time sampling described by a periodic data carrier term, $p(t)$, of period T_o,

$$d(t)=a(t)p(t)=\sum_{n=-\infty}^{\infty} a(nT_o)\delta(t\text{-}nT_o)=\frac{1}{T_o}\sum_{n=-\infty}^{\infty} a(nT_o)e^{j2\pi nt/T_o}$$

Because $a(t)$ and $p(t)$ are statistically independent we may again obtain the cyclic autocorrelation function from (3). Assuming $a(t)$ is purely stationary, noting that the Fourier transform of $p(t)$ consists of delta functions at harmonics of the symbol rate with amplitude $1/T_o$, and performing considerable algebraic manipulation yields,

$$S_d^{\alpha}(f)=\begin{cases} \dfrac{1}{T_o^2}\sum_{\lambda} S_a^{\alpha-\lambda}(f\text{-}\lambda\text{-}\dfrac{\alpha}{2}) & ;\alpha=\dfrac{k}{T_o}, \lambda=\dfrac{l}{T_o} \\ 0 & ;otherwise \end{cases}$$

5

where k and l are integers. It is observed that $d(t)$ is a basic component for many digital modulation formats, which suggests that the cyclic spectrum of $d(t)$ will appear in a number of other digital modulation examples.

2.1.2 QPSK

A QPSK waveform may be described by

$$x(t) = d_I(t)\cos(2\pi f_o t) - d_Q(t)\sin(2\pi f_o t)$$

with the data signals $d_I(t)$ and $d_Q(t)$ as described above for $d(t)$. The derivation of the cyclic spectrum for the QPSK signals follows a similar approach as for the PSK signal. Unlike the PSK example however, the cyclic autocorrelation for QPSK yields non-zero correlation only at the carrier frequency. The cyclic spectrum for $\alpha = \pm 2 f_o$ tends to zero when $d_I(t)$ and $d_Q(t)$ are balanced - the quadrature components cancel. Letting $d_I(t) = d_Q(t) = d(t)$, the QPSK cyclic spectrum may be described by

$$S_x^\alpha(f) = \frac{1}{2}\left(S_d^\alpha(f+f_o) + S_d^\alpha(f-f_o)\right)$$

where $S_d^\alpha(f)$ is as given for PSK.

2.1.3 FH/MFSK

From [14], the cyclic spectrum for multiple FH/MFSK hops can be obtained by first considering the case of a single hop,

$$x(t) = d(t)e^{-j2\pi f_1 t}$$

where $d(t)$ is as described for the PSK example except with $a(nT_o) = 0,1$. The cyclic spectrum is

$$S_x^\alpha(f) = \begin{cases} \dfrac{1}{\Delta t} T_h^2 Sinc^2\!\left((f+f_1)T_h\right); & \alpha = 0 \\ 0; & \text{otherwise} \end{cases}$$

where $T_h = $ *hop period*, $Sinc(x) = sin(\pi x)/(\pi x)$. The envelope of the cyclic spectrum is a $Sinc(x)$ function in α at the carrier frequency. For the case of multiple hops, a similar envelope is expected at each of the hop carrier frequencies along with a component at a cycle frequency equal to the difference in the hop carrier frequencies,

6

$$S_y^\alpha(f) = \begin{cases} \dfrac{1}{\Delta t} T_h^2 \left[Sinc^2 \left((f+f_1) T_h \right) + Sinc^2 \left((f+f_2) T_h \right) \right]; & \alpha = 0 \\ \dfrac{1}{\Delta t} T_h^2 Sinc^2 \left(\dfrac{(f_1+f_2) T_h}{2} \right) e^{-i2\pi \left(\frac{f_1+f_2}{2} \right) \delta t}; & \begin{array}{l} \alpha = \pm (f_1 - f_2) \\ \delta t = t_1 - t_2 \end{array} \\ 0; & \textit{otherwise} \end{cases}$$

However, the cyclic autocorrelation for any given hop or between any number of hops will be non-zero for a given (f_o, α_o) only for the duration of a hop. The cyclic spectrum thus tends to zero for increasing time window, Δt.

2.1.4 FH/PSK

The FH/PSK waveform is described by

$$x(t) = m(t) d(t) e^{-j2\pi f_1 t}$$

where $m(t) = \pm 1$ is the PSK data and $d(t) = 0,1$ is the hop on/off pulse as given above. From [14], the spectrum is described by

$$S_x^\alpha(f) = \frac{1}{T_h} \sum_{n,m} X_n X_m^* \delta\left(f + \frac{\alpha}{2} - nf_h \right) \delta\left(f - \frac{\alpha}{2} - mf_h \right)$$

where $X_i =$ Fourier coefficients of $x(t)$ evaluated over a hop period, (i.e. a time-limited BPSK signal). $S_x^\alpha(f)$ is only non-zero for cycle frequencies equal to integer multiples of the hop rate. As with the FH/MFSK case, the cyclic spectrum tends to zero for increasing Δt.

7

3.0 CYCLIC SPECTRAL DENSITY ESTIMATION

In practice, signals under consideration are defined over a finite time interval. As a result, the cyclic spectral density cannot be measured exactly. Estimates of the cyclic spectral density can be obtained via time- or frequency-smoothing techniques [3,8-10]. In this report, a time-smoothing approach is investigated where the estimate of the cyclic spectral density is given by the time-smoothed cyclic periodogram [3], $S_{x_{T_w}}^{\alpha}(t,f)_{\Delta t}$,

$$
S_x^{\alpha}(f) \approx S_{x_{T_w}}^{\alpha}(t,f)_{\Delta t} = \frac{1}{\Delta t} \int_{t-\Delta t/2}^{t+\Delta t/2} S_{x_{T_w}}(u,f)\,du
$$

$$
= \frac{1}{\Delta t} \int_{t-\Delta t/2}^{t+\Delta t/2} \frac{1}{T_w} X_{T_w}(u,f+\frac{\alpha}{2}) X_{T_w}^{*}(u,f-\frac{\alpha}{2})\,du \tag{5}
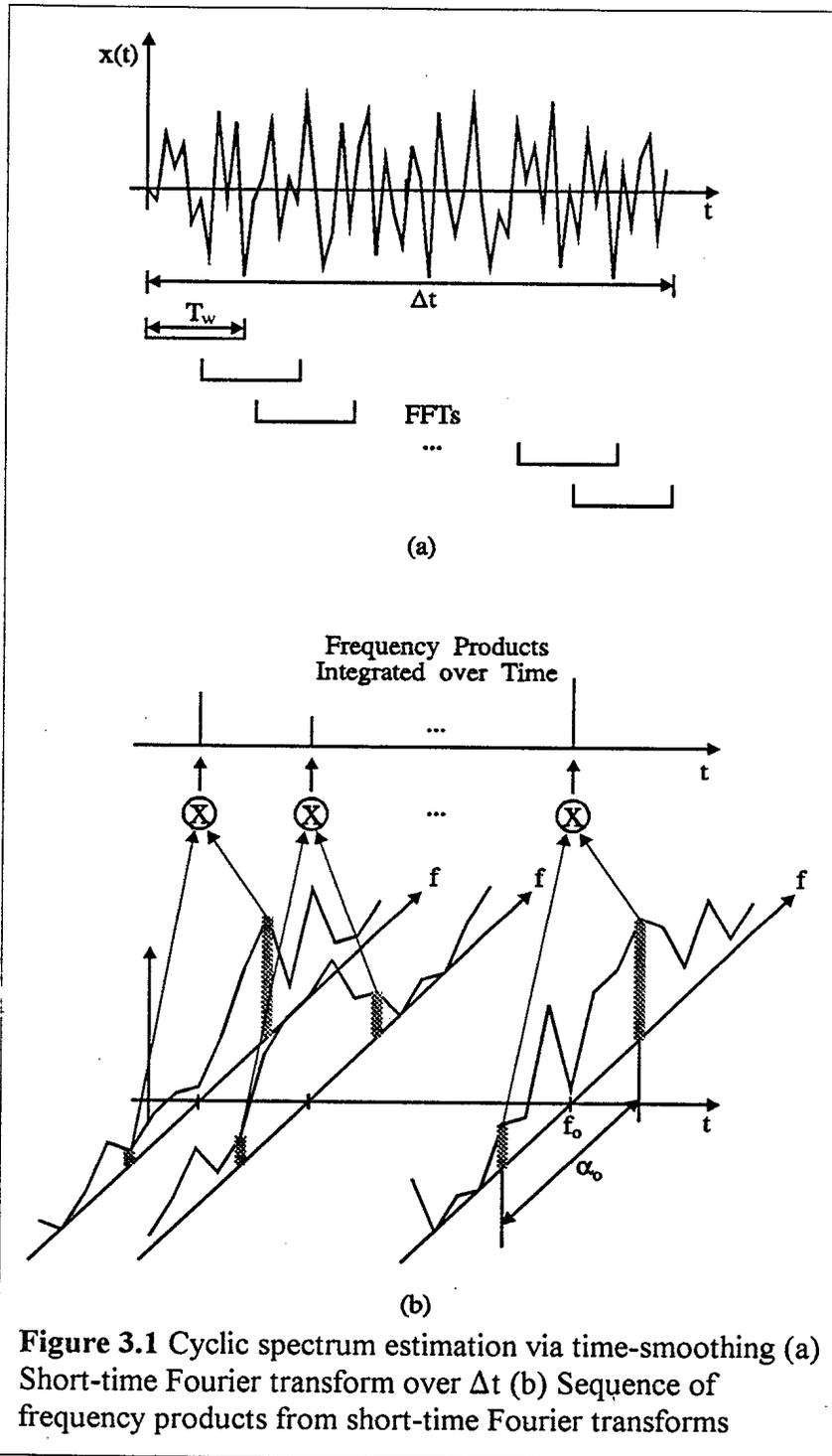$$

where $\Delta t = observation\ time$, $T_w = time\ window\ length$, and

$$
X_{T_w}(t,f) = short\ time\ Fourier\ transform\ of\ x(t)
$$

$$
\triangleq \int_{t-T_w/2}^{t+T_w/2} x(u)e^{-j2\pi fu}\,du \tag{6}
$$

Figure 3.1 illustrates this process graphically for an arbitrary (f_o, α_o). For some signal, $x(t)$, frequency components are evaluated over a time window, T_w, along the entire observation interval Δt. At each window, two components, centred about some f_o and separated by some α_o are multiplied and the resulting sequence of products is integrated over time.

Spectral components obtained from the short-time Fourier transform have a resolution, Δf, of approximately $1/T_w$. The product of two such components also provides a resolution capability in f of $1/T_w$ for the cyclic spectrum estimates. To minimize the effects of spectral and cyclic leakage introduced through frequency component sidelobes [10,14], a data taper window (e.g. Hamming window) is applied. Estimate reliability is further enhanced if a substantial amount of smoothing is carried out over Δt to reduce the variance of the estimate. From Grenander's Uncertainty Condition [3], this requires that

$$
\Delta t \Delta f \gg 1
$$

8

Figure 3.1 Cyclic spectrum estimation via time-smoothing (a) Short-time Fourier transform over Δt (b) Sequence of frequency products from short-time Fourier transforms

9

which means that the observation time must greatly exceed the time window used to compute the spectral components. Furthermore, it is shown [3] that the cycle frequency resolution of the estimate is $\Delta\alpha \approx {}^{1}/\Delta t$. This implies that an estimate for some (f_o, α_o) represents a very small area on the bifrequency plane (Figure 3.2) and to adequately represent the cyclic spectrum requires a significant number of estimates. It follows that using a brute force approach to obtain estimates is computationally demanding.

Figure 3.2 One cyclic spectrum estimate on a bifrequency plane for a lowpass signal
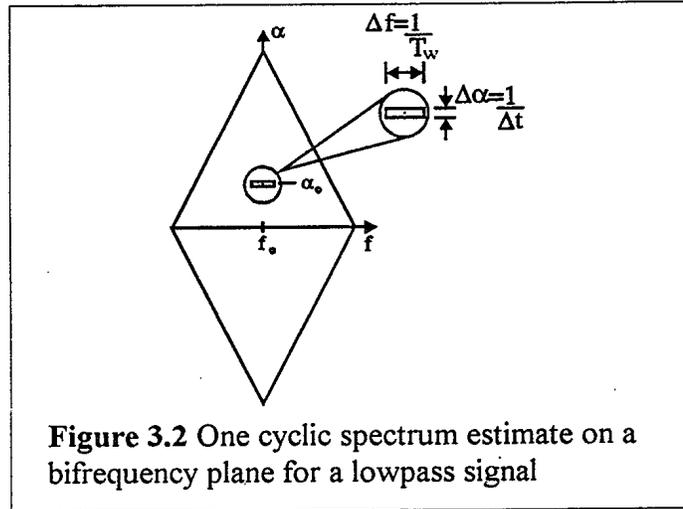
3.1 The FFT Accumulation Method

Computationally-efficient techniques for obtaining cyclic spectrum estimates have been developed to try to reduce the number of computations and are described in [9,10,14]. One particular algorithm based on the time-smoothing approach is called the FFT Accumulation Method (FAM). The strategy of the FAM algorithm is to divide the bifrequency plane into smaller areas called channel pair regions and compute the estimates a block at a time using the efficient FFT.

The first step in describing the FAM algorithm is to express **(5)** in discrete terms yielding,

$$S^{\gamma}_{x_{N'}}(n,k)_N = \frac{1}{N}\sum_n \frac{1}{N'} X_{N'}(n,k+\frac{\gamma}{2}) X^*_{N'}(n,k-\frac{\gamma}{2}) \tag{7}$$
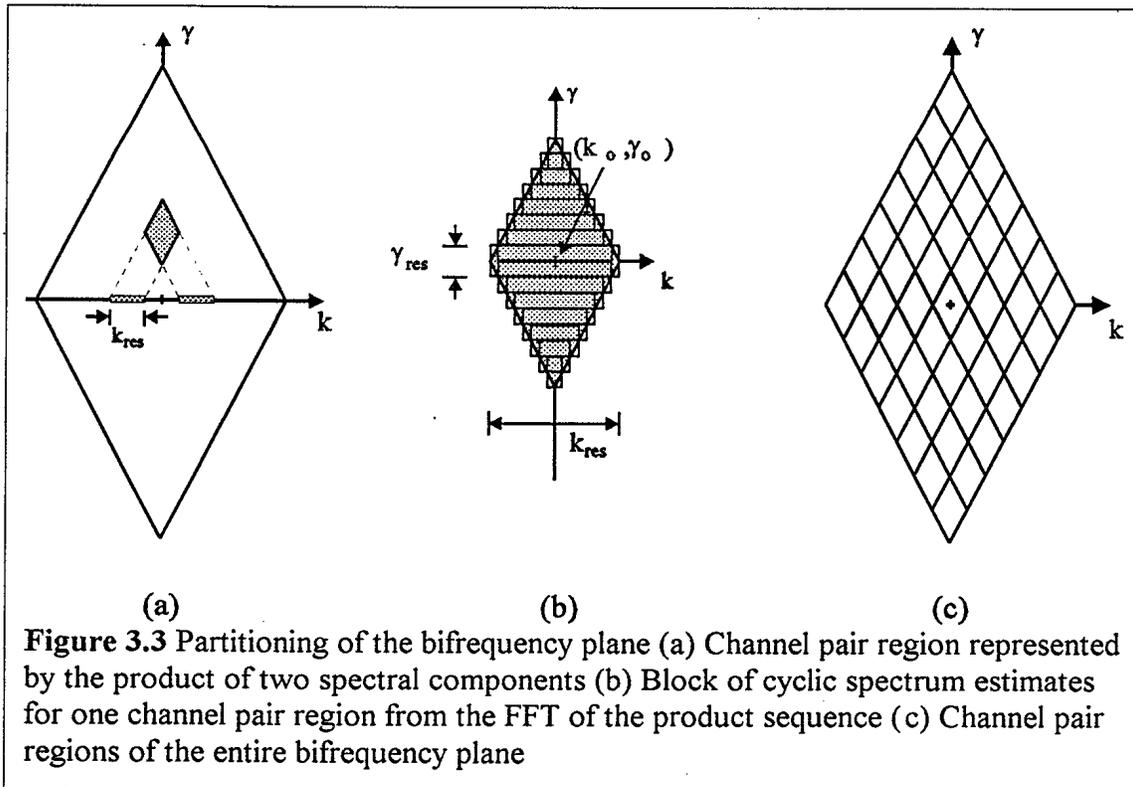
where

$$X_{N'}(n,k) \triangleq \sum_{n=0}^{N'-1} w[n]x[n]e^{\frac{-j2\pi kn}{N'}} \tag{8}$$

and $w[n]$= data taper window. The discrete equivalents of f and α are k and γ

respectively. Parameters N and N' represent the length of the sequence and length of the discrete short-time FFT. Extending Grenander's Uncertainty Condition, the reliability of the discrete estimate now depends on,

$$N/N' \gg 1$$

In the FAM algorithm, spectral components of a sequence, *x[n]*, are computed using **(8)**. Two components are multiplied to provide a sample of a cyclic spectrum estimate representing a finite area on the bifrequency plane called a channel pair region (Figure 3.3(a)). A sequence of samples for that particular area can be obtained by multiplying the same two components for a series of consecutive short-time FFTs which span the length of the input sequence. However, instead of computing an average of the product sequence, as in **(7)**, an FFT is performed on the second sequence to further resolve the estimates along the cycle frequency axis. The second FFT generates a block of cyclic spectrum estimates; one of these (i.e. the DC component) would include the estimate obtained by time-averaging (Figure 3.3(b)). Estimates for the entire cyclic spectrum are obtained by following this procedure for all combinations of spectral component pairs from the short-time FFTs (i.e. channel pair regions) as shown in Figure 3.3(c).

(a)   (b)   (c)

Figure 3.3 Partitioning of the bifrequency plane (a) Channel pair region represented by the product of two spectral components (b) Block of cyclic spectrum estimates for one channel pair region from the FFT of the product sequence (c) Channel pair regions of the entire bifrequency plane

11

From Figure 3.3(b), it is obvious that estimates toward the "top" and "bottom" of the channel pair region do not satisfy Grenander's Uncertainty Condition. To address this problem, one approach involves taking only those resolved cyclic spectrum components that are the equivalent in γ of $\pm k_{res}/2$ away from the centre of the channel pair region [10]. However, taking only some of the cyclic spectrum estimates will leave gaps in the bifrequency plane (Figure 3.4). This can be resolved by exploiting the effect of applying a data taper window in **(8)** on the frequency resolution to obtain better channel pair region coverage as shown in Figure 3.5.

Figure 3.4 Gaps in bifrequency plane when considering only estimates that are $\pm k_{res}/2$ away from the channel pair region centre
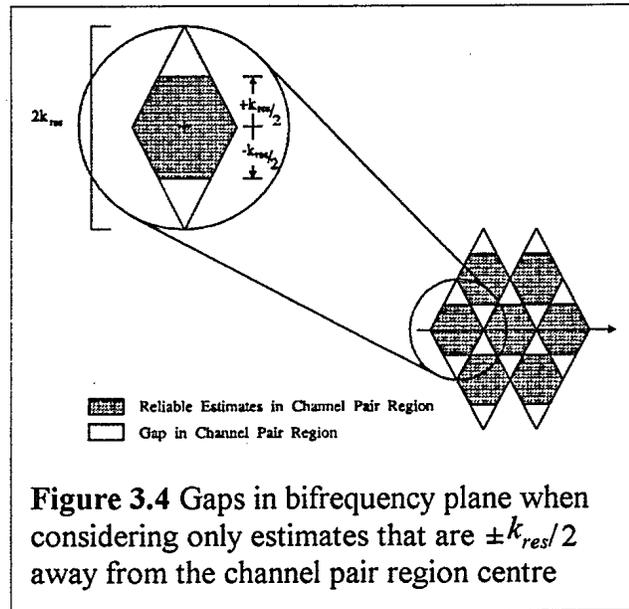
By computing a block of estimates using an efficient FFT, the number of computations is significantly reduced. Additional savings in computational requirements can be achieved by reducing the number of short-time FFTs. This is accomplished by decimating the product sequence and performing short-time FFTs every L samples instead of at every sample. The parameter L is referred to as the overlap parameter. It is shown [10,11,14] that to guard against aliasing and cycle leakage effects on the cyclic spectrum estimates, $L \leq N'/4$. A comparison of the computational requirements of the FAM algorithm show a reduction by a factor of N over a brute force approach [10,14].

12

Figure 3.5 Overlapping channel pair regions (a) with Hamming window (b) Channel pair region covered by estimates$\pm k_{res}/2$ from centre
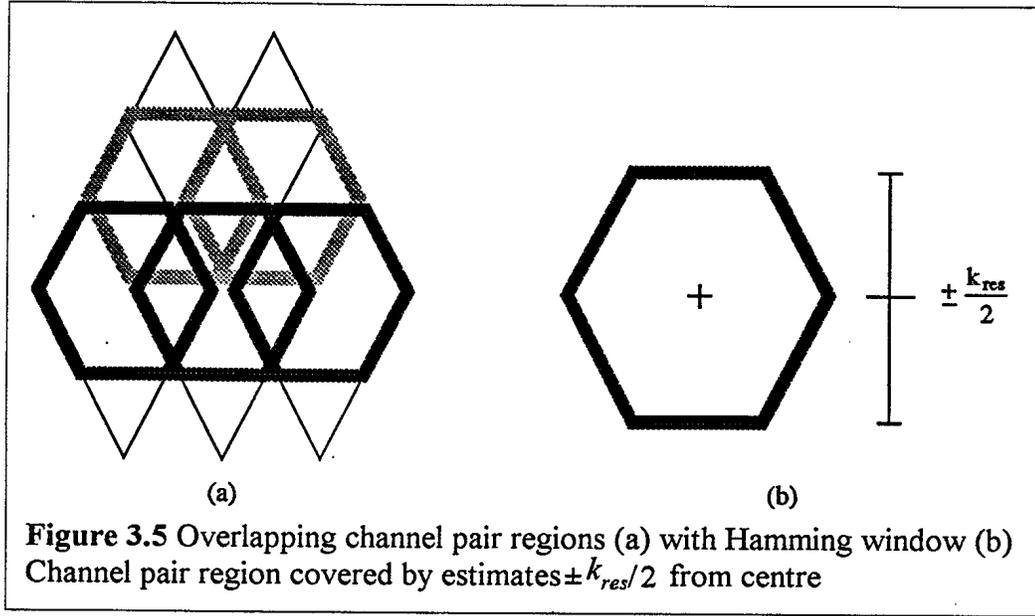
Taking into consideration the issues discussed above, the FAM algorithm can be expressed by the following,

$$S_{x_{N'}}^{\gamma_u+q\Delta\gamma}(n,k_v)_N = \sum_m \left[X_N(n+mL,k_v+\frac{\gamma_u}{2})X_N^*(n+mL,k_v-\frac{\gamma_u}{2})\ e^{\frac{-j2\pi\gamma_u mL}{N'}} \right] e^{\frac{-j2\pi mq}{P}}$$

(9)

where,

$$X_{N'}(r,k)= \sum_{a=0}^{N'-1} w[a]x[a+r]e^{\frac{-j2\pi ka}{N'}} \qquad ,w[a]=window\ coefficients$$

(10)

and P = length of the product sequence.

13

4.0 IMPLEMENTATION AND TEST SETUP

The purpose of this section is to present the components of the experimental setup used to test an implementation of the FAM algorithm. The FAM algorithm was implemented on a PC/c5x DSP board made by Loughborough Sound Images Inc. The DSP board includes a Texas Instruments TMS320c51 DSP chip which performs the FAM computations. A general description of the implementation is included.

4.1 Experimental Setup

The key components in the experimental setup are as follows: signal generation, received signal processing, baseband signal processing and data collection, cyclic spectrum estimate computation, and hardware/user interface. They are illustrated in Figure 4.1.
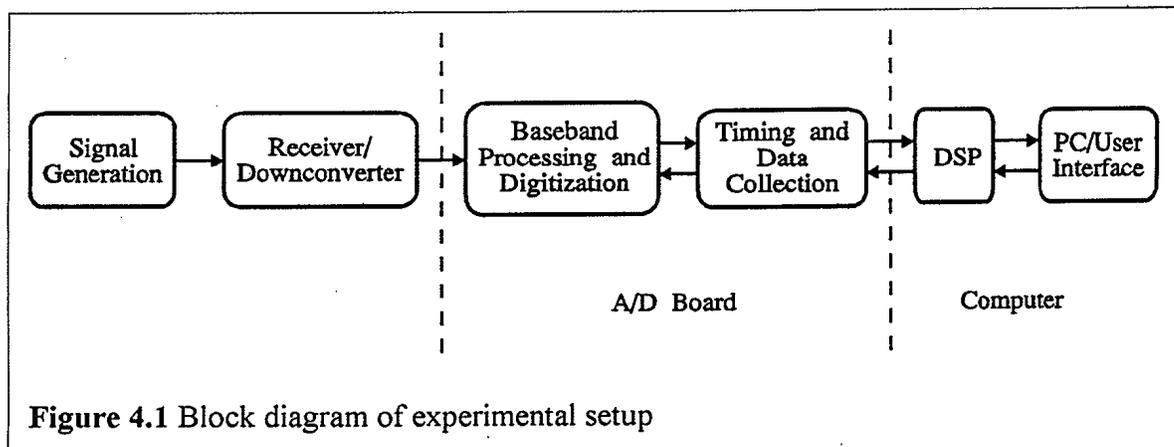
Figure 4.1 Block diagram of experimental setup

In order to simplify the setup without affecting the evaluation of the FAM algorithm, input test signals are generated at IF and combined. In effect, these signals represent a typical front end of a communications receiver. The resulting signal is translated via quadrature detection, producing the I and Q baseband signals to be analyzed. An analog-to-digital (A/D) board collects, digitizes and stores the input waveform. At the command of the DSP, the stored waveform is read into DSP memory for the FAM computations. Further details on each one of these blocks are described in [14].

14

4.2 FAM implementation description

4.2.1 FAM computations overview

The FAM algorithm was implemented in assembler for the TMS320c51 DSP board made by Loughborough Sound Images, Inc. The assembler program is divided into three modules: data pre-processing, computation of frequency components, and computation of cyclic spectrum estimates. A flow chart showing the main functions of the assembler program according to these three modules is given in Figure 4.2. In this report, a summary of the computational process is presented. Specific details, however, are contained in [14].

At the start of the assembler program for the FAM computations, parameters including the input sequence length (N =1024), short-time Fourier transform length (N'=32), and overlap parameter (L = 8) are initialized. A master reset of the A/D board is initiated by the DSP. When the DSP receives a ready signal from the A/D board, the data collected on the A/D board is read into DSP board memory. A/D samples are represented as 12-bit signed numbers using offset binary coding and need to be converted to 2's complement representation for the DSP computations. In this implementation, the input sequence is zeropadded so that the length of the second sequence, P, will be a power-of-2 to facilitate the use of a Radix-2 FFT routine.

A series of overlapping short-time FFTs is performed to obtain the spectral components of the input sequence. The output of each short-time FFT is stored in an array. All frequency components are normalized to 16 bits to reduce the memory requirements when products are subsequently formed from these frequency components and stored.

Complex product sequences for a particular channel pair region at (k_o, γ_o) are formed by multiplying the appropriate spectral components together over all the short-time FFTs or time hops. For each product, a time-shift exponential factor is applied to preserve the coherence of the spectral components between successive short-time FFT hops. A second FFT is performed on the product sequence to obtain the cyclic spectrum estimates for that channel pair region. As described in Section 3.1, only estimates representing the area $\pm k_{res}/2$ away from the centre of the channel pair region are retained to maintain statistical reliability. These estimates are then stored in DSP memory. This process is repeated for all possible combinations of spectral components or channel pair regions. The DSP then sends a signal to the PC to indicate that the cyclic spectrum estimates are ready to be transferred. It is noted [10] that since the product sequences and the second FFT calculations in the third module are independent of one another, they can be implemented in parallel, thus saving some computation time.

15

4.2.2 DSP/PC Handshaking

The DSP board is contained in an IBM-compatible PC and interfaces to the PC through I/O and memory-mapped (status and control) registers. The PC loads the DSP program and resets the DSP board to start the FAM computations. When the DSP indicates that the computations have been completed, the PC transfers and formats the results of the FAM computations, and produces an ASCII file of the formatted output.
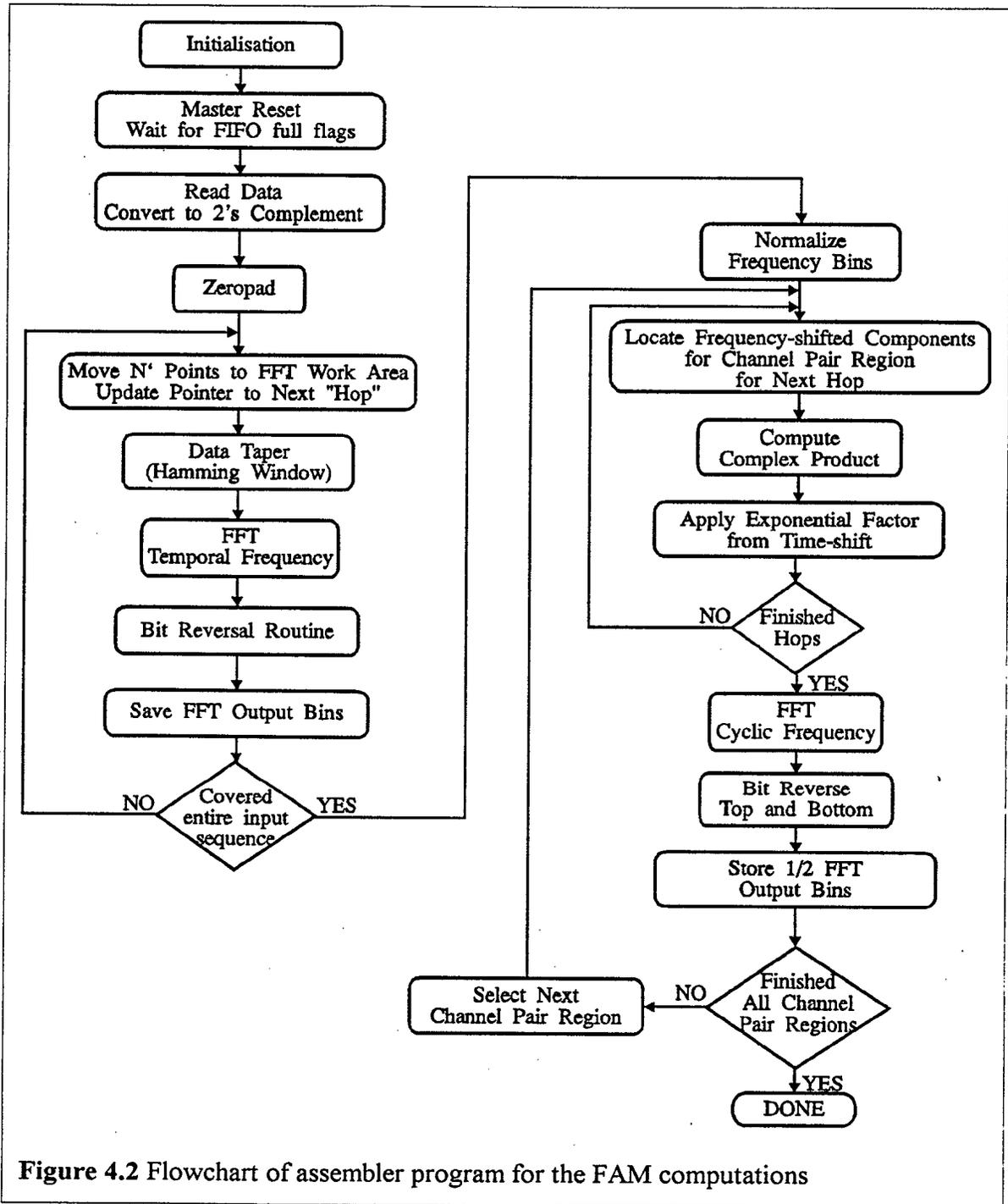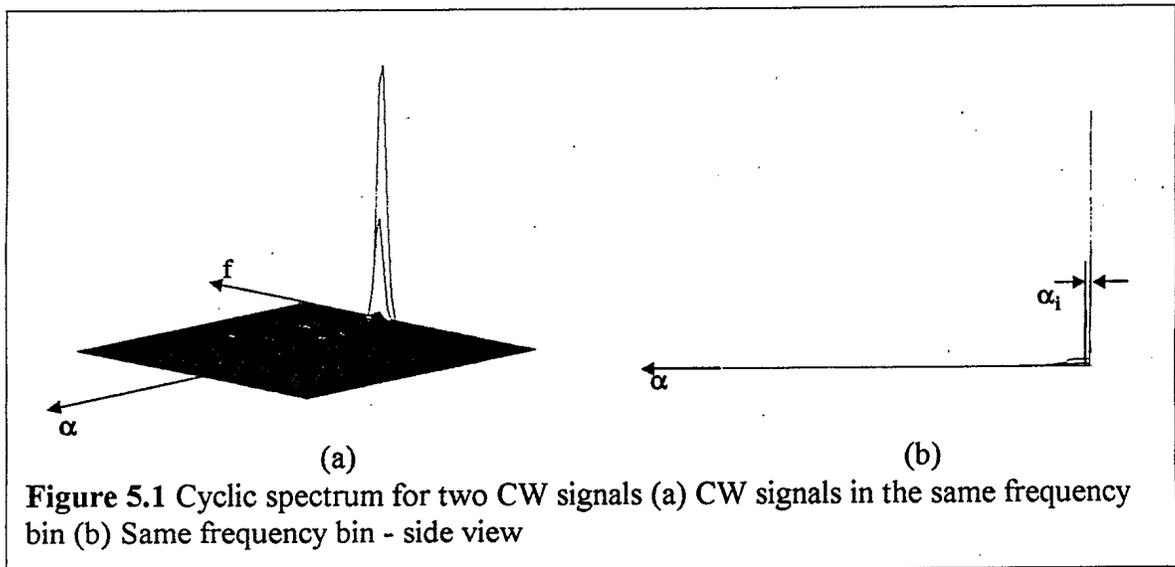
Figure 4.2 Flowchart of assembler program for the FAM computations
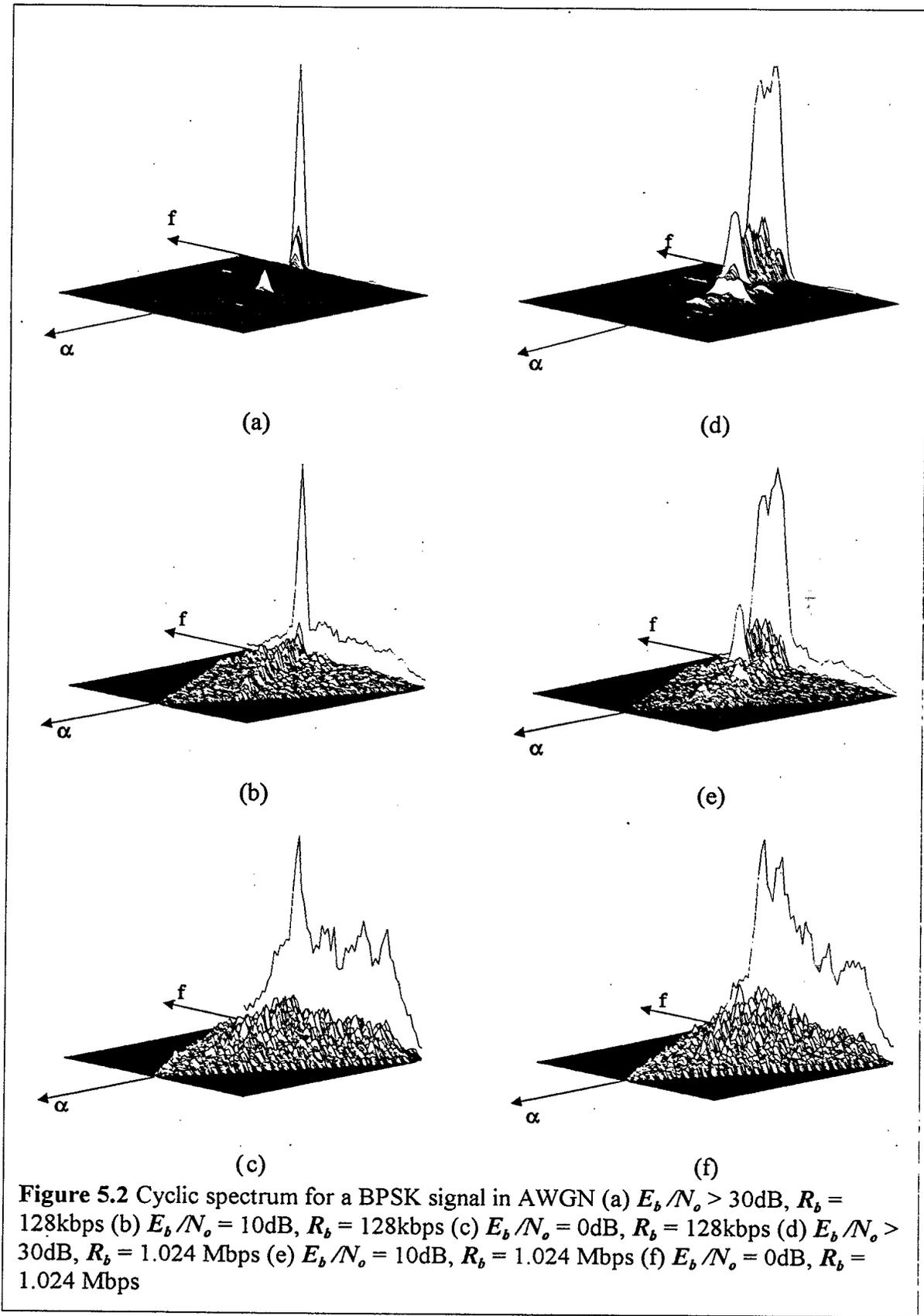
17

5.0 EXPERIMENTAL RESULTS

Using the FAM implementation described in the previous sections, the cyclic spectrum was estimated for different cases of experimental and simulated input data. The results are presented for some common modulation schemes including BPSK, QPSK, FH/MFSK, and FH/PSK.

To verify the implementation of the FAM algorithm, two CW signals, with carrier frequencies close to one another, were generated as the input signal. Figure 5.1 illustrates the resulting cyclic spectrum. A cyclic component is observed at α_i which corresponds to the difference between the two carrier frequencies. This illustrates the potential for cyclic spectral analysis to be used to detect two or more signals within the same band of interest where it would be difficult using the conventional power density spectrum (along $\alpha = 0$).

Figure 5.1 Cyclic spectrum for two CW signals (a) CW signals in the same frequency bin (b) Same frequency bin - side view

For BPSK waveforms, a comparison of the cyclic spectra for low and high data rate signals in AWGN is given in Figure 5.2. From the PSK example of Section 2.1.1, a cyclic component at the data is expected. The low data rate BPSK signal, however, shows no distinguishable component in the cyclic spectrum. With the relatively short input sequence length implemented ($N = 1024$) compared to the symbol period, there was not enough signal captured to obtain an accurate estimate for small values of α. This result illustrates that using as large an observation time window as is practical would be preferred for detection applications. In the case of the higher data rate signal, a cyclic component is visible as more data symbols are included in the calculation for the same observation time owing to the shorter bit period.

18

Figure 5.2 Cyclic spectrum for a BPSK signal in AWGN (a) $E_b/N_o > 30$dB, $R_b = 128$kbps (b) $E_b/N_o = 10$dB, $R_b = 128$kbps (c) $E_b/N_o = 0$dB, $R_b = 128$kbps (d) $E_b/N_o > 30$dB, $R_b = 1.024$ Mbps (e) $E_b/N_o = 10$dB, $R_b = 1.024$ Mbps (f) $E_b/N_o = 0$dB, $R_b = 1.024$ Mbps

The cyclic spectrum for a QPSK waveform was computed and is shown in Figure 5.3. The symbol rate of the signal is exhibited in the bifrequency plane. However, no spectral correlation associated with the carrier frequency is observed as in the case of the BPSK waveform (Figure 5.3(a)). As noted in Section 2.1.2, this component is cancelled out by the in-phase and quadrature components of the QPSK waveform which allows the two modulation schemes to be distinguished from one another. The non-zero values surrounding the cyclic component are related to the variance of the estimate for the relatively short input sequence.

Figure 5.3 Cyclic spectrum for BPSK and QPSK waveforms (a) Real BPSK signal, $R_b=1.024Mbps$ (b) Real QPSK signal, $R_s=512ksps$
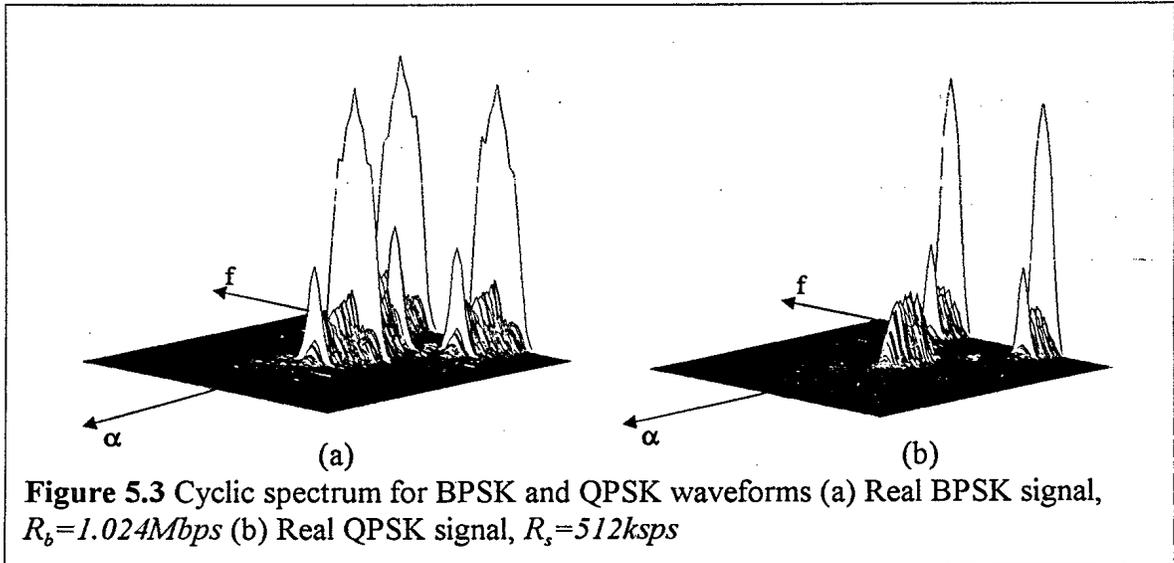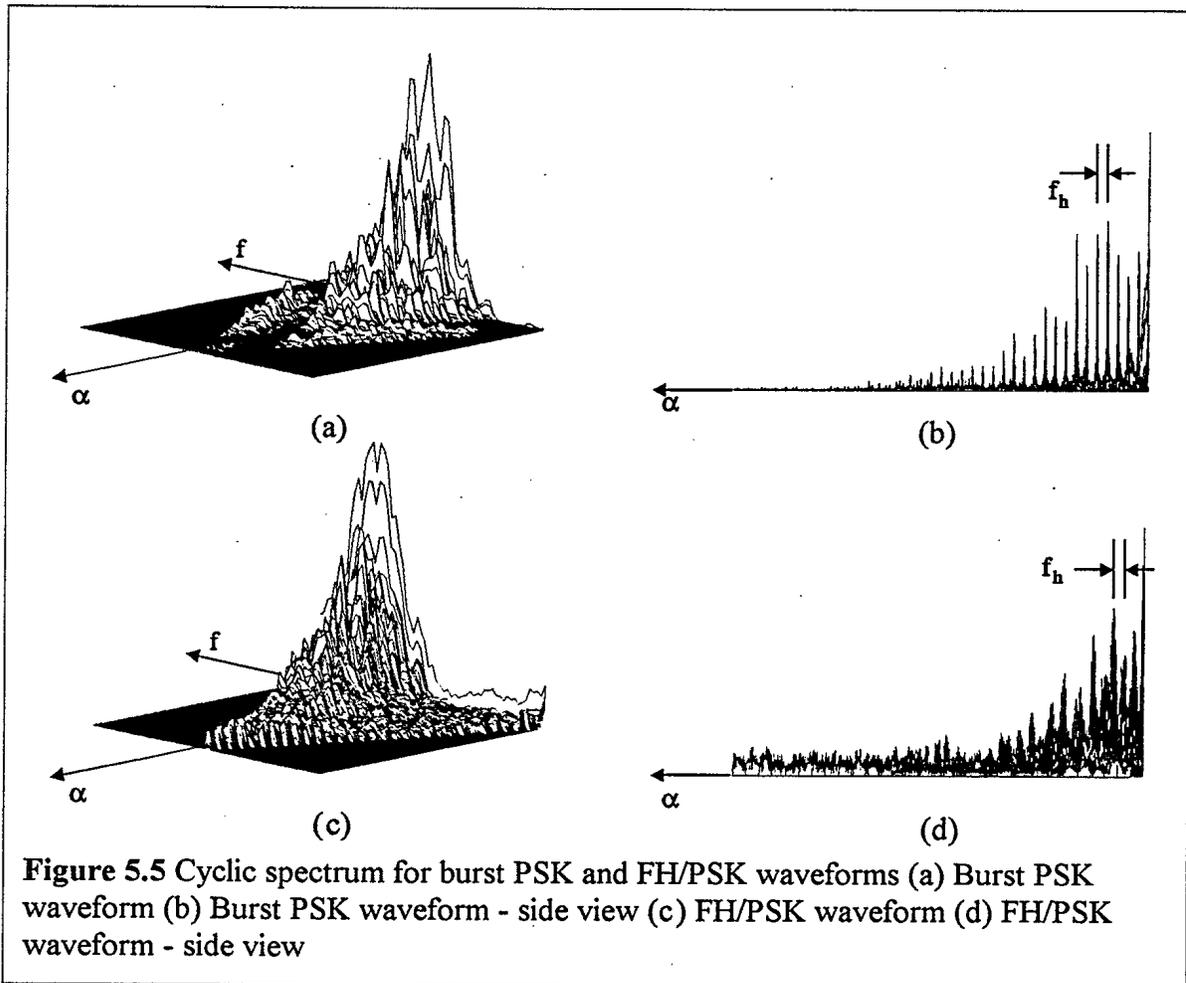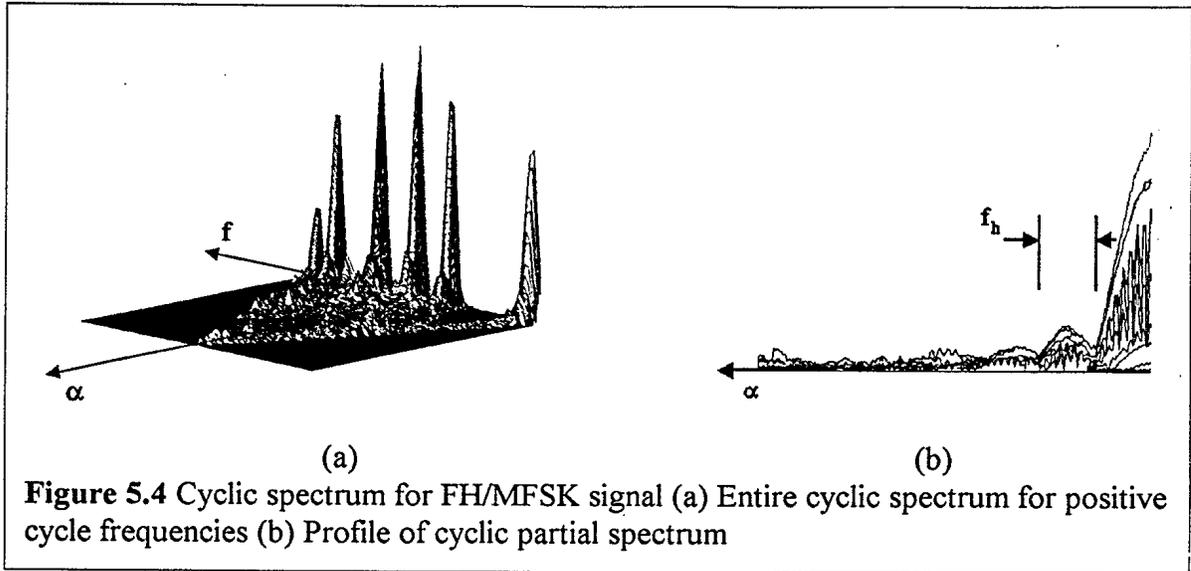
Figure 5.4 shows the cyclic spectrum computed for an FH/MFSK signal. There are several hops observed in the frequency band of interest in the form of distinct peaks along the $\alpha =0$ axis. However, no spectral correlation is observed between the carrier frequencies of the hops, as was suggested in Section 2.1.3, because in this example, only one transmission over a particular hop period is received. As a result, when the overlapping short-time FFTs are computed in the FAM algorithm, two or more frequency hops are unlikely to be captured simultaneously. Consequently, the only non-negligible products in the second sequence are those centred about the individual hops. However, for multiple transmissions over a hop period, correlation would also be observed at a cycle frequency equal to the difference in carrier frequency.

Similar cyclic spectra are observed in Figure 5.5 for FH/PSK and burst PSK waveforms. Although Figures 5.5(a) and 5.5(c) do not reveal any distinct cyclic features, the profiles show the periodic component of the signal, the hop rate. The cyclic components of the FH/PSK example appear "noisier" than in the burst PSK example due to the fact that they are computed from a single hop. The profile also shows the effect of the superposition of the $Sinc^2$-like amplitude response function associated with the Fourier transform of the hop data.

20

Figure 5.4 Cyclic spectrum for FH/MFSK signal (a) Entire cyclic spectrum for positive cycle frequencies (b) Profile of cyclic partial spectrum

Figure 5.5 Cyclic spectrum for burst PSK and FH/PSK waveforms (a) Burst PSK waveform (b) Burst PSK waveform - side view (c) FH/PSK waveform (d) FH/PSK waveform - side view

21

6.0 SUMMARY AND CONCLUSIONS

Cyclostationary spectral analysis is a technique which exploits the periodicities inherent in digitally-modulated signals and enables signals with overlapping temporal spectra to be isolated at their cycle frequency. It involves treating the signal under examination as a cyclostationary rather than stationary process. The basic equations for cyclostationary spectral analysis (i.e. the cyclic autocorrelation and cyclic spectral density) are reviewed. Cyclic spectra are evaluated for typical Satcom signals including PSK and spread spectrum waveforms.

Techniques for estimating the cyclic spectrum are derived from time- and frequency-smoothing approaches. Obtaining high reliability estimates, however, requires significant computational resources. This report considers a time-smoothing approach and examines the key components of the computationally-efficient FAM algorithm. The reduction in the number of computations is attributed to the use of an FFT to compute cyclic spectrum estimates a block at a time as well as decimation and data taper windowing considerations. The FAM algorithm is implemented on a TMS320c5x DSP in three main processes: data pre-processing, computation of frequency components, and computation of cyclic spectrum estimates. The DSP is then used to compute the cyclic spectra of BPSK, QPSK, FH/MFSK, and FH/PSK waveforms.

Theoretical and FAM estimates of the cyclic spectrum have demonstrated the technique's ability to identify typical Satcom waveforms. Periodic components such as the carrier frequency, symbol rate and hop rate are exhibited in the form of distinct cycle frequency components in the bifrequency plane. Results also indicate that two or more signals could be detected within the same band of interest. Further improvements in estimate reliability for this implementation can be achieved by increasing the observation time, though at the expense of computation time. However, this can be overcome by considering parallel implementations of the third process in the FAM algorithm. This, along with advances in computing power and algorithm development would enhance the potential of cyclostationary spectral analysis to be a practical tool for detection and identification.

22

REFERENCES

1.   Proceedings of the 19th Meeting of TTCP Subgroup S Technical Panel STP-6 Space Communications, Workshop on *"Response of Satellite Communications Systems to Stress"*, Volumes V-A and V-B, October-November 1991.

2.   Gardner, W.A., "The Spectral Correlation Theory of Cyclostationary Time-series", *Signal Processing*, vol. 11, no. 1, pp.13-36, July 1986.

3.   Gardner, W.A., *Statistical Spectral Analysis: A Non-probabilistic Theory*, Prentice-Hall, N.J., 1987.

4.   Benson, T.A., "Geolocation of an Electromagnetic Emitter Using a Cyclostationary Time-Difference-of-Arrival Technique", Master's Thesis, Naval Postgraduate School, Monterey, CA, December 1992.

5.   Gardner, W.A., "Signal Interception: A Unifying Theoretical Framework for Feature Detection", *IEEE Transactions on Communications*, vol.36, no.8, pp.897-906, August 1988.

6.   Gardner, W.A., Spooner, C.M., "Signal Interception: Performance Advantages of Cyclic Feature Detectors", *IEEE Transactions on Communications*, vol.40, no.1, pp.149-159, January 1992.

7.   Gardner, W.A., Spooner, C.M., "Cyclic Spectral Analysis for Signal Detection and Modulation Recognition", *Proceedings of the IEEE Military Communications Conference*, San Diego, CA, pp.24.2.1-24.2.6, October 1988.

8.   Gardner, W.A., "Exploitation of Spectral Redundancy in Cyclostationary Signals", *IEEE Signal Processing Magazine*, pp.14-36, April 1991.

9.   Gardner, W.A., "Measurement of Spectral Correlation", *IEEE Transactions on Acoustics, Speech, and Signal Processing*, vol. ASSP-34, no.5, pp.1111-1123, October 1986.

10. Roberts, R.S., Brown, W.A., Loomis Jr., H.H., "Computationally-efficient Algorithms for Cyclic Spectral Analysis", *IEEE Signal Processing Magazine*, pp.38-49, April 1991.

11. Mudry, A.H., "The Exploitation of Spectral Correlation for the Purpose of Signal Search and Detection", DSTO Research Note ERL-0572-RN, Salisbury, Australia, September 1991.

12.   April, E., "On the Implementation of the Strip Spectral Correlation Algorithm for Cyclic Spectrum Estimation", DREO Technical Note 94-2, Ottawa, Canada, February 1994.

13.   Brousseau, N., Salt, J.W.A., "Real-time Analysis of a Spread Spectrum Environment with an Optoelectronic Cyclic Cross Correlator: Proof-of-concept experiments"., DREO Technical Note (to be published), Ottawa, Canada.

14.   Tom, C., "Investigation and Implementation of a Computationally-efficient Algorithm for Cyclic Spectral Analysis", Master's Thesis, Ottawa-Carleton Institute for Electrical Engineering, Carleton University, Ottawa, Canada, March 1995.

LIST OF SYMBOLS AND ABBREVIATIONS

A/D	Analog-to-Digital
AWGN	Additive White Gaussian Noise
BPSK	Binary-Phase-Shift-Keyed
CDMA	Code Division Multiple Access
CW	Continuous Wave
dB	Decibel
DSP/PC	Digital Signal Processor/Personal Computer
E_b/N_o	Bit-energy-to-noise-spectral-density ratio
f	Temporal frequency
FAM	FFT Accumulation Method
FFT	Fast Fourier Transform
FH/MFSK	Frequency-Hopped/M-ary Frequency-Shift-Keyed
FH/PSK	Frequency-Hopped/Phase-Shift-Keyed
k	Discrete cycle frequency
$kbps$	Kilobits-per-second
k_{res}	Discrete temporal frequency resolution
L	Overlap parameter
$Mbps$	Megabits-per-second
n	Discrete time variable
N	Discrete length of observation interval
N'	Discrete length of short-time Fourier transform
P	Length of product sequence
PSK	Phase-Shift-Keyed
QPSK	Quadrature-Phase-Shift-Keyed
R_b	Data bit rate
$R_x^\alpha(\tau)$	Cyclic autocorrelation function
$Sinc(x)$	Sinc function, $Sinc(x)=sin(\pi x)/(\pi x)$
$S_x^\alpha(f)$	Cyclic spectral density or cyclic spectrum
$S_{x_{N'}}^\gamma(n,k)_N$	Discrete time-smoothed cyclic periodogram
$S_{x_{T_w}}^\alpha(t,f)_{\Delta t}$	Time-smoothed cyclic periodogram
TDOA	Time-Difference-of-Arrival
TTCP	The Technical Cooperation Program
T	Arbitrary time interval
T_h	Hop period
T_w	Time window
$x(t)$	Continuous time signal
$X_{N'}(n,k)$	Discrete short-time Fourier transform
X_i	Fourier coefficients of a signal $x(t)$

25

$X_T(f)$	Fourier transform over an interval T
$X_{T_w}(t,f)$	Short-time Fourier transform of $x(t)$
$w[n]$	Discrete data taper window
α	Cycle frequency
γ	Discrete cycle frequency
γ_{res}	Discrete cycle frequency resolution
$\Delta\alpha$	Cycle frequency resolution
Δf	Frequency resolution
Δt	Observation time interval

SECURITY CLASSIFICATION OF FORM
(highest classification of Title, Abstract, Keywords)

DOCUMENT CONTROL DATA
(Security classification of title, body of abstract and indexing annotation must be entered when the overall document is classified)

1. ORIGINATOR (the name and address of the organization preparing the document. Organizations for whom the document was prepared, e.g. Establishment sponsoring a contractor's report, or tasking agency, are entered in section 8.) Defence Research Establishment Ottawa Ottawa, Ontario K1A 0Z4	2. SECURITY CLASSIFICATION (overall security classification of the document including special warning terms if applicable) UNCLASSIFIED

3. TITLE (the complete document title as indicated on the title page. Its classification should be indicated by the appropriate abbreviation (S,C or U) in parentheses after the title.)

Cyclostationary Spectral Analysis of Typical Satcom Signals using the FFT Accumulation Method (U)

4. AUTHORS (Last name, first name, middle initial)

Tom, C.

5. DATE OF PUBLICATION (month and year of publication of document) December 1995	6a. NO. OF PAGES (total containing information. Include Annexes, Appendices, etc.) 35	6b. NO. OF REFS (total cited in document) 14

7. DESCRIPTIVE NOTES (the category of the document, e.g. technical report, technical note or memorandum. If appropriate, enter the type of report, e.g. interim, progress, summary, annual or final. Give the inclusive dates when a specific reporting period is covered.)

DREO Report

8. SPONSORING ACTIVITY (the name of the department project office or laboratory sponsoring the research and development. Include the address.

9a. PROJECT OR GRANT NO. (if appropriate, the applicable research and development project or grant number under which the document was written. Please specify whether project or grant) Project 05C01	9b. CONTRACT NO. (if appropriate, the applicable number under which the document was written)

10a. ORIGINATOR'S DOCUMENT NUMBER (the official document number by which the document is identified by the originating activity. This number must be unique to this document.) DREO REPORT 1280	10b. OTHER DOCUMENT NOS. (Any other numbers which may be assigned this document either by the originator or by the sponsor)

11. DOCUMENT AVAILABILITY (any limitations on further dissemination of the document, other than those imposed by security classification)

(X) Unlimited distribution
( ) Distribution limited to defence departments and defence contractors; further distribution only as approved
( ) Distribution limited to defence departments and Canadian defence contractors; further distribution only as approved
( ) Distribution limited to government departments and agencies; further distribution only as approved
( ) Distribution limited to defence departments; further distribution only as approved
( ) Other (please specify):

12. DOCUMENT ANNOUNCEMENT (any limitation to the bibliographic announcement of this document. This will normally correspond to the Document Availability (11). however, where further distribution (beyond the audience specified in 11) is possible, a wider announcement audience may be selected.)

Unlimited Announcement

SECURITY CLASSIFICATION OF FORM

RA.W (24 Nov 93)

-28-

13. ABSTRACT (a brief and factual summary of the document. It may also appear elsewhere in the body of the document itself. It is highly desirable that the abstract of classified documents be unclassified. Each paragraph of the abstract shall begin with an indication of the security classification of the information in the paragraph (unless the document itself is unclassified) represented as (S), (C), or (U). It is not necessary to include here abstracts in both official languages unless the text is bilingual).

The suitability of cyclostationary spectral analysis for the detection and identification of typical Satcom signals is examined. An overview of the general equations for cyclostationary spectral analysis is presented. The cyclic spectrum is derived for some common Satcom modulation schemes. Cyclic spectrum estimation techniques are described with particular emphasis on the time-smoothed approach. Key aspects of a computationally-efficient algorithm for computing the cyclic spectrum estimates, called the "Fast Fourier Transform (FFT) Accumulation Method" (FAM) are outlined. The FAM algorithm is implemented on a Digital Signal Processor/Personal Computer (DSP/PC) board containing a TMS320c51 processor chip and used to compute the cyclic spectrum for various phase-shift-keyed (PSK) and spread spectrum waveforms. The results are presented and discussed.

14. KEYWORDS, DESCRIPTORS or IDENTIFIERS (technically meaningful terms or short phrases that characterize a document and could be helpful in cataloguing the document. They should be selected so that no security classification is required. Identifiers, such as equipment model designation, trade name, military project code name, geographic location may also be included. If possible keywords should be selected from a published thesaurus. e.g. Thesaurus of Engineering and Scientific Terms (TEST) and that thesaurus-identified. If it is not possible to select indexing terms which are Unclassified, the classification of each should be indicated as with the title.)

cyclostationary spectral analysis
computationally-efficient algorithms
cyclic spectrum
signal processing
cyclic autocorrelation
Satcom
cyclic spectral density
FFT Accumulation Method
statistical analysis

155037